Available online at www.sciencedirect.com
SCIENCE DIRECT®
Proceedings of the Combustion Institute 30 (2005) 1591–1599
Proceedings of the Combustion Institute
www.elsevier.com/locate/proci

UV absorption of CO_2 for temperature diagnostics of hydrocarbon combustion applications

J.B. Jeffries[a,*], C. Schulz[b,1], D.W. Mattison[a], M.A. Oehlschlaeger[a], W.G. Bessler[b], T. Lee[a], D.F. Davidson[a], R.K. Hanson[a]

[a] *High Temperature Gasdynamics Laboratory, Mechanical Engineering Department, Stanford University, Stanford, CA 94305-3032, USA*
[b] *PCI, Universität Heidelberg, Heidelberg, Germany*

Abstract

At room temperature, CO_2 is transparent in the ultraviolet (UV) at wavelengths longer than 205 nm; however, at temperatures above 1000 K the CO_2 absorption cross-section becomes significant in the region between 200 and 320 nm. Because CO_2 is a major product of hydrocarbon combustion and because both the magnitude of the absorption cross-section and the shape of the UV absorption spectrum vary strongly with temperature, measurements of UV optical absorption spectra offer the potential to infer gas temperature in combustion systems. In this paper, we demonstrate the first use of UV absorption measurements to determine temperature using five different experimental examples to illustrate the utility in hydrocarbon combustion applications of this new temperature diagnostic strategy. (1) Transmission measurements of cw laser light at 266 nm are used to determine time-resolved temperature in shock-heated CO_2. (2) Similar transmission measurements are used to infer time-resolved temperature behind a detonation wave in a pulse-detonation engine using absorption from equilibrium concentrations of the CO_2 combustion product. (3) The absorption of pulsed laser light near 226 nm is used to infer temperature in the burned gases of a premixed high-pressure methane flame. (4) Wavelength-resolved absorption of light from a broadband UV deuterium lamp is time-resolved with a kinetic spectrograph to acquire time-resolved absorption spectra illustrating the measurement of temperature in a system with changing temperature and CO_2 mole fraction. (5) Time-gated, spectrally resolved transmission of a deuterium lamp is used to derive temperature at specific crank angles in a piston engine. These examples demonstrate that temperature measurements based on UV optical absorption of CO_2 have good potential for use in a wide variety of hydrocarbon combustion applications.

Keywords: Absorption; Optical absorption; Temperature; Combustion diagnostics

1. Introduction

At the 29th Combustion Symposium, we reported that the ultraviolet absorption of hot CO_2 could be a significant interference for laser-based diagnostics measurements in the ultraviolet (UV) between 200 and 300 nm [1]. Strong

* Corresponding author. Fax: +650 723 1748.
E-mail address: Jay.Jeffries@Stanford.edu (J.B. Jeffries).
[1] Current address: Institut für Verbrennung und Gasdynamik, Universität Duisberg-Essen, Lotharstrasse 1, 47057 Duisberg, Germany.

1540-7489/$ - see front matter
doi:10.1016/j.proci.2004.08.009

attenuation of laser and signal light was observed during in-cylinder NO laser-induced fluorescence (LIF) imaging measurements in the burned gases of gasoline and Diesel-fired piston engines [2–4] as well as in high-pressure flames [5]. The initial hypothesis that hot CO_2 was the primary absorber [6] was confirmed by the measurement of the relatively large CO_2 absorption cross-section in the range 200–320 nm in shock-heated gases at 900–3050 K [7]. UV-excitation of CO_2 gives rise to broadband CO_2 LIF [8], which for hydrocarbon combustion effluent can interfere with NO-LIF measurements [9]. Photodissociation into CO and O has been reported to cause strong interference with two-photon LIF measurements of O-atoms [10].

In this paper, we identify the opportunity to infer temperature (T) from the UV absorption of CO_2 in hot combustion products. A new temperature measurement strategy is proposed and demonstrated for combustion applications that exploit the T-dependence of the reported CO_2 absorption cross-sections. CO_2 is a major product of hydrocarbon combustion, and thus is present in significant quantities in the hot burned gases. For many practical systems, the pressure and the feedstock gas composition are known, and the CO_2 concentration is in chemical equilibrium; for such a system, we demonstrate that a measurement of the UV attenuation at a single wavelength can be used to determine the temperature. However, both the magnitude of the absorption cross-section and the shape of the absorption spectrum vary with temperature. Thus, in systems with unknown CO_2 concentration, temperature can be determined via attenuation measurements at two or more wavelengths.

Measurement of T from UV absorption of CO_2 provides a new diagnostic tool complementing other laser-based optical techniques. Like other absorption methods the most straightforward application provides path-integrated temperature. Such measurements do not have the spatial resolution offered by LIF; however, absorption-based measurements provide high-speed realtime measurements with the potential for control applications, and the optical access requirements are modest offering the potential for measurements in production engines or industrial applications. The CO_2 absorption diagnostic discussed here is most applicable to high temperatures at high pressure, which is a regime where other optical methods (especially LIF) have great difficulty. The CO_2 absorption signal is strongest at high T, and thus is relatively immune to the interference from the dense, cold boundary layers that are a problem for Rayleigh and Raman methods.

Five examples are considered to illustrate the potential of CO_2 absorption measurements to determine gas temperature in combustion applications. First, we examine the transmission of a continuous (cw) laser near 266 nm across a CO_2/argon (Ar) mixture in a shock tube. At temperatures below 3000 K, the time-resolved attenuation measurement captures the variation in gas temperature caused by non-ideal shock tube processes after the end of the typical test time. The second example uses similar time-resolved attenuation of a 266 nm cw laser to infer the gas temperature in the burned gases behind a detonation wave in a pulse detonation engine. The third example illustrates that the attenuation of pulsed UV light, near typical NO excitation wavelengths of 226 nm, can be used to infer temperature in the burned gases of a high-pressure premixed methane/air flame. In this system, the pressure and the feedstock gas composition are known, and the CO_2 concentration is in thermal equilibrium in the burned gases of this flame. The laser attenuation is observed at right angles via spatial variations in NO-LIF signal intensities within an area of homogeneous NO concentrations. The fourth example uses time-resolved absorption spectra from CO_2/Ar mixtures using a deuterium (D_2) lamp and a kinetic spectrograph in a shock tube. The gas temperature is determined from the shape of the absorption spectrum without reliance on the chemical composition of the gas. The fifth example measures wavelength-resolved attenuation of light from a D_2 lamp to infer the crank-angle-resolved gas temperature in a propane-fired piston engine. These five examples show this new temperature strategy has potential for time-resolved gas temperature measurements in a wide variety of hydrocarbon combustion applications. Before discussing the individual applications, the background photophysics of the T-diagnostics is discussed.

2. The temperature measurement strategy

Optical absorption of light at wavelength λ and intensity I_0 by a mole fraction X_i of species i in a gas of density n at pressure p can be written:

$$I(\lambda) = I_0(\lambda) \times \exp\left(-\int_0^l \sigma_i(\lambda,T)X_i(T,x)n(p,T,x)\,\mathrm{d}x\right), \quad (1)$$

where I is the transmitted intensity, σ_i is the absorption cross-section (a function of λ and T), and in general X_i and n vary with position along the path dx with total length l.

For CO_2, the cross-section σ was fit in the range 200–320 nm and 900–3050 K to a semi-empirical form: $\ln \sigma_{CO_2}(\lambda,T) = a + b\lambda$, where $a = c_1 + c_2T + c_3/T$ and $b = d_1 + d_2T + d_3/T$. The cross-section is given in units 10^{-19} cm^2 with T, in 1000 K, λ, in 100 nm, and $c_1 = 17.2456$, $c_2 = -3.1813$,

$c_3 = 0.8836$, $d_1 = -7.0094$, $d_2 = 1.6142$, and $d_3 = -3.1777$ [1]. This semi-empirical form is consistent with the physical picture of optical absorption to a bent electronic excited state of CO_2. Because CO_2 has a linear ground state, the Franck–Condon principle would only allow significant absorption from CO_2 molecules with excited bending vibrations. Thus, the lower state of the absorption is not the ground state, and the absorption cross-section has an Arrhenius-like "activation energy" for population in the excited absorbing level.

For measurements in examples 1–3 below, except for a thin cold boundary layer, p, T, and X_{CO_2} are all constant over the path length, the number density is expressed as an ideal gas ($pV = nRT$), and the absorbance A_λ becomes:

$$A_\lambda = \ln\left(\frac{I_0(\lambda)}{I(\lambda)}\right) = X_{CO_2}(T)\frac{pV}{RT} l\sigma(T,\lambda). \quad (2)$$

For known CO_2 concentrations and p, the measured absorbance at a single wavelength can be directly used to infer T. Figure 1 shows A_λ versus T for a 2% CO_2 mixture at 1 bar for a 15 cm path length. If the CO_2 is generated by combustion (examples 2 and 3), an iterative approach may be used to extract T that produces the observed absorbance while calculating the T-dependent CO_2 equilibrium concentration.

The shape of the CO_2 absorption spectrum also varies with T. This makes it possible to determine the temperature from wavelength-resolved absorbance measurements. The T-dependent shape is illustrated in Fig. 2, where the logarithm of absorption cross-section is plotted versus wavelength. Note that these semi-log plots are nearly linear with a slope that varies with T. This can be analytically understood using the semi-empirical form of the cross-section from Eq. (2). For this discussion, we assume an isothermal, isobaric, uniform gas mixture (i.e., p, T, and X_{CO_2} are independent of x) in a cell of length l. From Eqs. (1) and (2) and:

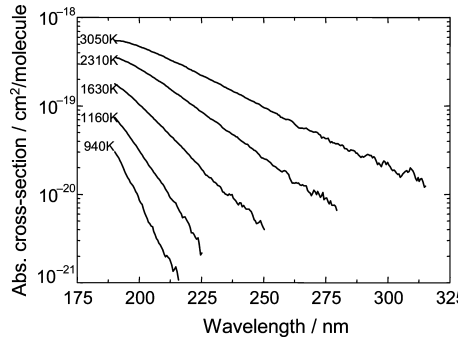

Fig. 2. CO_2 optical absorption cross-section versus wavelength for 5 temperatures (940, 1160, 1630, 2310, and 3050 K) measured in shock-heated CO_2/Ar mixtures.

$$A_\lambda = X_{CO_2}\frac{pV}{RT} l \exp\left(a(T) + b(T)\lambda\right), \quad (3)$$

which can be rewritten as:

$$\ln(A_\lambda) = \ln\left(\ln\left(\frac{I_0(\lambda)}{I(\lambda)}\right)\right) = \ln\left(X_{CO_2}\frac{pV}{RT} l\right) + a(T) + b(T)\lambda.$$

Thus, at a given temperature, the logarithm of the fractional transmission is linear in λ with a slope defined by $b(T) = d_1 + d_2T + d_3T$ (see Fig. 3). Therefore, T can be directly inferred from Fig. 3 and the measured slope of a plot of $\ln(A_\lambda)$ versus λ. Once T has been determined, the value of A_λ at any wavelength can be used to calculate X_{CO_2} independent of equilibrium assumptions.

The path integral along the total absorption path l makes the problem much more difficult, because even for an isobaric application with uniform mixing of combustion products, T often varies along the path. Chemical equilibrium can often be assumed for the combustion product mole fraction. In practical applications, cold

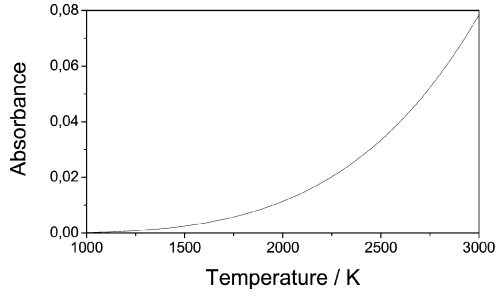

Fig. 1. Absorbance expected from Eqs. (2) and (3) for 2% CO_2 in argon across (15.24 cm) the shock tube at 266 nm from 1000 to 3000 K.

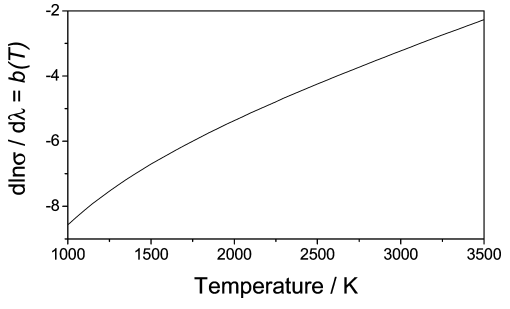

Fig. 3. $d(\ln(\sigma))/d\lambda = b(T)$ versus temperature; this is the expected slope of the observed absorption by CO_2 as a function of temperature as described in the text.

boundary layers can have a disproportionate influence on the measured absorption because the density $n = pV/RT$ is largest in the cold boundary layer, and the mole fraction of a final combustion product is maximized at the lowest T. However, for UV absorption by CO_2, the absorbance is strongly weighted by the T-dependence of σ, which is largest at the highest T (mitigated by thermal decomposition of CO_2 at $T > 3000$ K). Furthermore, the technique presented in example 3 does not use line-of-sight integration and therefore allows temperature measurements in subsections of the laser beam (i.e., the stable inner area of the flame neglecting the fluctuating boundaries).

3. Results

The use of UV attenuation by hot CO_2 is now used to infer gas temperature in five test examples. The first three examples use attenuation of a single wavelength and known CO_2 concentration to determine T, and the next two examples use the shape of the CO_2 absorption spectrum to infer T without relying on known CO_2 concentration. In three of these examples (1, 3, and 4), the expected temperature is well understood and provides a good test of this new diagnostic strategy. Using these examples to validate the measurement technique, the temperature is then measured in less well-understood engine experiments (3 and 5), where the inferred time-resolved temperature is a good illustration of the use of this diagnostic strategy for practical applications.

3.1. Example 1: Time-resolved temperature in shock-heated gas mixtures

A mixture of 2% CO_2 diluted in argon is heated by a gas-driven incident shock and subsequent reflected shock, providing a nearly stationary, isothermal gas sample. The experiment is performed in a high-purity, turbo-pumped, stainless steel shock-tube (15.24 cm diameter) that has been extensively used for measurements of chemical reaction rates [11]. Initial reflected shock wave conditions were calculated from measured incident shock speeds using standard ideal-gas shock wave relations [12]. Figure 4 shows these ideal pressure and temperature (p_5 and T_5) conditions as straight lines at 0.876 bar and 2867 K. For this gas mixture and reflected-shock T, there is no appreciable CO_2 thermal decomposition. The pressure is measured by a high-speed piezo-electric transducer (cf. Fig. 4). After 2 ms, a pressure rise to ~1.0 bar is observed. This pressure rise originates from an interaction of the reflected shock with the contact surface between the driver gas (He) and the test gas mixture. For the non-reactive gas mixture, T can be calculated from the measured pressure trace assuming an isentropic process.

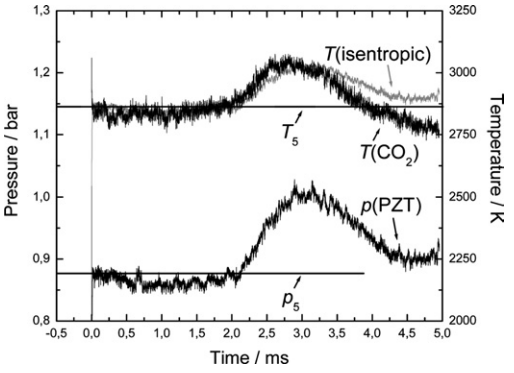

Fig. 4. Time-resolved temperature and pressure measured in shock-heated mixture of 2% CO_2 in Ar. Time zero is the arrival of the reflected shock. The horizontal lines mark the T_5 and p_5 temperature and pressure expected from shock heating of ideal gas.

The attenuation of 266 nm cw laser light by the heated CO_2 is used to infer time-resolved T after the reflected shock passes (time zero in Fig. 4). The output of a frequency-doubled, diode-pumped, cw Nd:YAG (Coherent, 5 W@532 nm) is doubled in an external BBO crystal providing ~1 mW of light at 266 nm. This laser light passes un-attenuated across the shock tube in the room temperature test gas, but undergoes ~2.5% attenuation after the reflected shock passes. The observed attenuation together with the measured p and the T-dependent CO_2 absorption cross-section provides gas temperature with 1 μs time-resolution that agrees with the ideal gas T-prediction within 1% at time zero. The resulting T agrees (±30 K) with the simulated T until approximately 3.5 ms after the shock when the isentropic assumption breaks down. The measurement in Fig. 4 illustrates the use of CO_2 absorption to extract precise time-resolved gas temperature.

3.2. Example 2: Time-resolved temperature in a pulse detonation engine

The attenuation of the 266 nm cw laser in the combustion gases behind a detonation wave in a pulse detonation engine (PDE) provides time-resolved gas T as shown in Fig. 5. The experiment is performed in the Stanford PDE that is 3.8 cm in diameter and 160 cm in length and instrumented with a variety of optical access, pressure, and ion probe ports [13–15]. The tube is fueled at 1 bar with premixed, stoichiometric C_2H_4/O_2 as monitored with a tunable diode laser sensor [16]. The 266 nm laser absorption is measured 144 cm from the head end of the tube; there is no attenuation prior to the detonation wave,

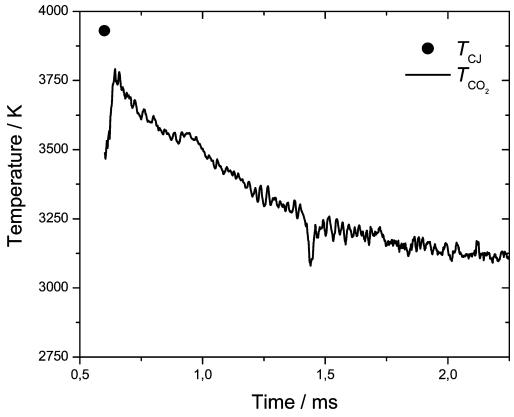

Fig. 5. Time-resolved gas temperature in the gases behind a detonation wave in a stoichiometric C_2H_4/O_2 mixture. The point denotes the CJ value.

and significant attenuation is observed after the detonation wave arrives, and p and T rise to Chapman–Jouguet (CJ) values of ~40 bar ~3930 K. This temperature exceeds the temperature range for which CO_2 absorption cross-section data are reported in Ref. [2], and are outside the valid T-range of Eq. (2) [1]. Therefore, the needed high-T (3000–4500 K) CO_2 absorption cross-section was measured at 266 nm in a shock tube with known CO_2 concentrations. Variations in CO_2 concentration due to thermal decomposition were taken into account by extrapolating the measured attenuation to $t = 0$. These new cross-section data will be reported separately in a more comprehensive study of CO_2 quantitative spectroscopy [17].

The peak T inferred from CO_2 absorption in the PDE is 3850 K; given the difficulties of optical measurements disrupted by the passage of a detonation wave (and a pressure change from 1 to 40 bar) and the large values of 266 nm absorbance, we consider this measurement to be in good agreement with the Chapman–Jouguet prediction. A second laser beam near 390 nm where the gas is transparent is used to account for the beam steering by the denotation wave. Pressure is independently measured using a pressure transducer. Note, the absorption-based T is an absolute measurement, which does not rely on any calibration; only the assumption that the CO_2 concentration is in chemical equilibrium. Finite rate chemical modeling suggests that the CO_2 concentration in the post-detonation gases reaches equilibrium with a sub-μs time constant, thus confirming the use of an equilibrium assumption to reduce the 266 nm absorption data. Figure 5 shows the time-resolved measurements as the pressure drops from the Chapman–Jouguet's value to ~3 bar, and T drops to ~3000 K. There is good agreement between recent computational model predictions and measurements of T [18].

3.3. Example 3: Temperature in high-pressure premixed methane/air flames

We have extensively studied high-pressure NO-LIF diagnostic strategies in premixed methane/air flames at pressures between 1 and 60 bar [5,9,19,20]. In these experiments, attenuation by CO_2 absorption is an important correction for both the excitation laser energy (near 226, 237, and 248 nm) and the subsequent NO-LIF signal (at 225–260 nm). Despite the small size of the flame (8 mm exit diameter), the total reduction in LIF signal was up to 43% at 60 bar for the combination of 226 nm excitation and detection at 237 nm. From previous experiments, it is known that the burned gases form a symmetric stable cone with homogeneous T and concentration above the matrix that is surrounded by a slowly fluctuating boundary area. Figure 6 shows a raw image of NO-LIF at 60 bar. The observed

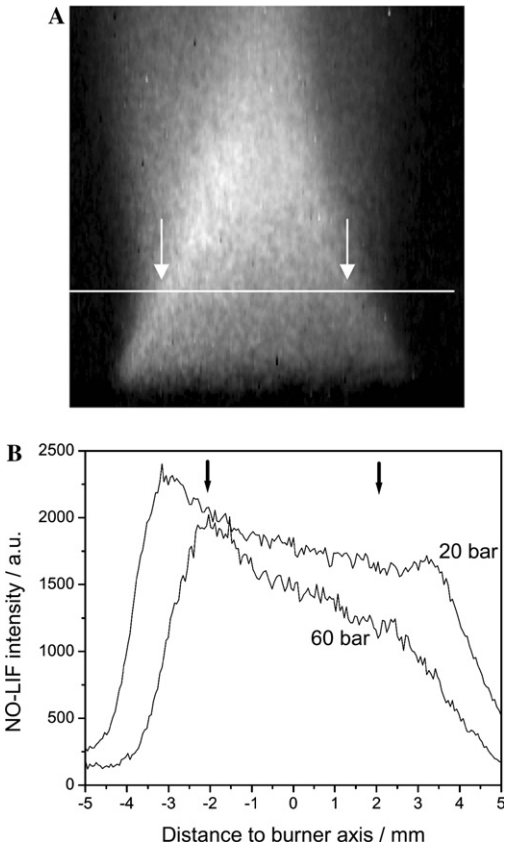

Fig. 6. Laser and signal light attenuation in NO-LIF measured in a 60 bar high-pressure flame [5]. Excitation at 226 nm, detection at 230–240 nm. (A) NO-LIF intensity at 60 bar. (B) Intensity variation as a function of distance to the burner axis at 3 mm above the burner matrix. The positions used for the attenuation measurement are marked with arrows.

asymmetry in the NO-LIF images is due to attenuation of laser and signal light. The right frame in Fig. 6 shows a horizontal trace of the NO-LIF signal 3 mm above the burner matrix. The attenuation of the laser light is measured in the inner, stable zone only by extracting the NO-LIF intensities from two points at equal distance from the burner axis ($x = \pm 2$ mm). Due to the symmetry of the flame, signal attenuation is identical for both positions and needs not to be included in the evaluation. The laser attenuation caused by 300 ppm NO is <3% of the attenuation due to CO_2 at equilibrium concentrations and flame temperature [5], and thus NO absorption can be neglected in the data evaluation. From the variation in signal intensity between the two points, together with the T-dependent CO_2 absorption cross-sections and the assumption of chemical equilibrium concentrations, we obtain 2125, 2030, and 1880 K for the 20, 40, and 60 bar flames, respectively. This is in reasonable agreement with (slightly intrusive) measurements (2050, 1990, and 1945 K) by two-color pyrometry of a platinum bead suspended in the middle of the flame 3 mm above the burner matrix. The decrease in T with increasing p is consistent with the observed decrease in distance between burner matrix and flame front and hence, increasing heat-transfer to the burner matrix. Although T in the burned gas cone of this premixed flame is uniform within the measurement uncertainties, this NO-LIF imaging scheme illustrates the potential to measure spatially resolved laser attenuation with modest resolution. Compared to line-of-sight transmission measurements, this method has the advantage of avoiding boundary effects.

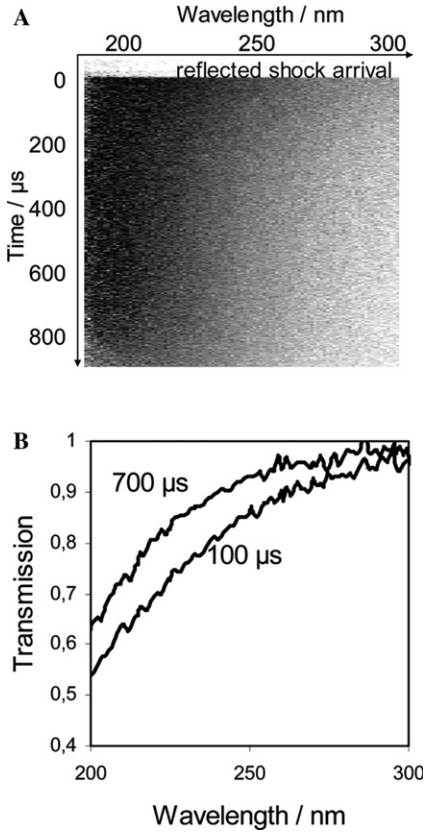

Fig. 7. (A) Absorption spectrum versus time for a D_2 lamp transmitted across a shock-heated CO_2/Ar mixture with T_5 3550 K. (B) Absorption spectrum for CO_2, 100 and 700 µs after shock heating.

3.4. Example 4: Temperature from CO_2 absorption spectra in shock-heated mixtures

The use of a broadband UV light source offers the potential to determine gas T from the shape of the CO_2 absorption spectrum (cf. Section 2). For this example, we direct light from a D_2 lamp across the shock tube used above (Section 3.2). The transmitted light is dispersed in an imaging spectrometer (Acton $f = 150$ mm $f/4$) and detected on an un-intensified CCD camera (Roper Scientific, EEV57); one dimension of the CCD image is wavelength, and the frame transfer feature makes time the second dimension (see Fig. 7A). The camera has a mask covering all but the first five rows of pixels. Using a shift rate of 2 µs per row, each row has a total exposure time of 10 µs, and thus wavelength-resolved transmission spectra can be acquired with 10 µs time resolution. This experimental method was used in [7] to obtain the CO_2 cross-section, and the experimental details are presented there. As shown in that work, if we shock-heat CO_2/Ar mixtures at temperatures below 2800 K there is negligible thermal decomposition, and when the absorption conditions do not change with time the signal-to-noise can be enhanced by averaging 1–2 ms of wavelength-resolved data (averaging many CCD rows). Data before the arrival of the shock wave provide I_0 enabling conversion of the spectral transmission data to fractional transmission data, and hence an absorption spectrum.

Figure 8 shows the results of 20 shock tube experiments on CO_2/Ar mixtures; the abscissa plots the ideal post-reflected-shock temperature T_5 determined from shock speed, and the ordinate plots of T determined by the shape of the CO_2 absorption spectrum. Note that none of these data were used in the earlier determination of the CO_2 absorption cross-section to generate the parameters of Eq. (2) [1,7]. For the data below 2800 K, the signal is averaged for 1 ms; for eight higher T-points, only the first 100 µs of data is considered and extracted from the kinetic spectrograph image. Six of these points are at T greater than our previous cross-section measurements, and thus, the increase in scatter of the data at these resulting

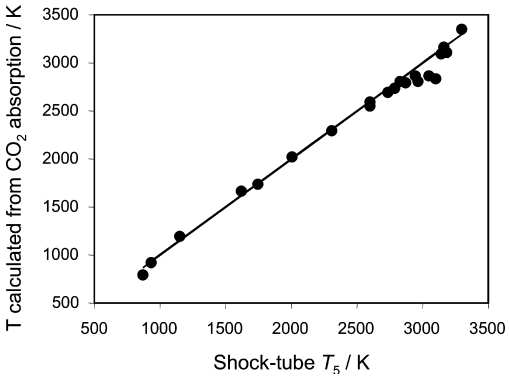

Fig. 8. Temperature recovered from the shape of the measured absorbance spectrum of a D_2 lamp transmitted across shock-heated CO_2/Ar mixtures versus the T_5 temperature expected after the reflected shock.

CO_2-absorption temperatures is not unexpected. The unity slope of the data in Fig. 8 validates the use of absorption spectrum shape to determine T.

Figure 7A is the kinetic spectrograph image of the highest temperature experiment with T_5 3550 K. This T is high enough that significant amount of CO_2 thermally decomposes during the measurement time shown in Fig. 7A. This decomposition lowers T as seen in the change of shape between the spectra shown in Fig. 7B at $t = 0.1$ and 0.7 ms. This change of shape in the absorption cross-section is interpreted as a change in temperature of nearly 600 K over a 600 μs measurement time as illustrated in Fig. 9. Thus, the shape of the CO_2 absorption cross-section can be used to determine T independently of a known CO_2 concentration. In the past, most shock-tube studies have been carried out under very dilute conditions to minimize the change in T because this T-change has not been readily measurable.

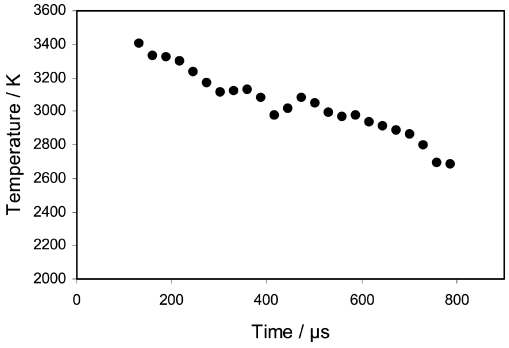

Fig. 9. Temperature determined by the shape of the CO_2 absorption spectrum versus time after reflected shock heating of a CO_2/Ar mixture from the data in Fig. 7; the cooling is caused by thermal decomposition of the CO_2.

The time-resolved T-measurement based on time-resolved CO_2 absorption-spectra measurements has the potential to overcome this limitation, for example in ignition delay studies.

3.5. Example 5: Crank-angle-resolved temperature in a piston engine

As illustrated in Section 3.4, T can be inferred from the shape of the CO_2 absorption spectrum. Here, this method is used to determine T in a piston engine; a D_2 lamp provides broad-band UV light that is directed across a single-cylinder optical engine [4]. The skip-fired engine was fueled on propane/air at 1000 rpm. The transmitted light was dispersed with an imaging spectrometer (Acton Spectra-Pro-275) and detected on a time-gated intensified CCD camera (Princeton Instruments). Figure 10 shows the transmission spectra for three different crank angles (CA): 1, 10, and 30° CA after top dead center (TDC) taken with 100 μs resolution (1.7° CA). The ignition timing is set to 20° CA before TDC. We assume a cylindrical shape of the flame, which is consistent with earlier Rayleigh scattering T-measurements in the same engine [21]. As determined from spatially resolved absorption measurements [4], at 361° CA the flame diameter, and hence the absorption length, is 2.5 cm; at 370° CA, the flame has almost propagated to the cylinder wall (7.0 cm path length); and at 390° CA, the burned gases fill the entire cylinder (7.5 cm diameter).

Examination of Fig. 10 shows that CO_2 and OH absorption can explain the shape of the observed optical transmission. The shape of the transmission for wavelengths less than 275 nm is dominated by CO_2 absorption. We calculate the wavelength-dependent transmission based on the temperature and wavelength-dependent CO_2 absorption cross-sections, measured in-cylinder pressures and equilibrium CO_2 concentrations for the $\phi = 1.0$ flame. The crank-angle-resolved T is determined within 50 K assuming homogeneous in-cylinder T by manually fitting the simulated curves to the observed transmission spectra. The crank-angle-dependent variation in in-cylinder pressure and temperature shown in Fig. 10 is consistent with the expectations for the operating conditions of this research engine. Thus, wavelength-resolved UV transmission shows excellent promise for crank-angle-resolved in-cylinder temperature measurements in research engines with optical access using fuels that do not absorb in the UV or with observation times where the fuel is completely burned.

4. Conclusions

The T-dependence of CO_2 absorption in the UV is used for the first time to determine gas

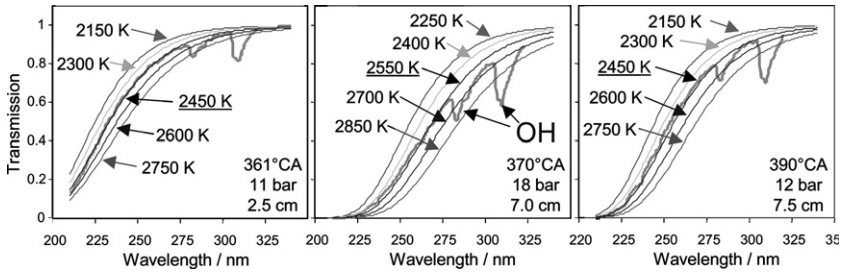

Fig. 10. Transmission spectrum for a D_2 lamp taken from a propane-fueled single-cylinder optical engine at three crank angles [6]. Predicted transmission in the presence of hot CO_2 is used to determine in-cylinder gas temperature.

temperature. Five experimental demonstration experiments are conducted to illustrate the potential for precise, time-resolved, *T*-measurements in the burned gases of hydrocarbon combustion applications. Three examples (1–3) use the attenuation of the transmission of a single laser wavelength and a known CO_2 concentration to extract time-resolved temperature. One example (4) uses only the wavelength-resolved shape of the absorbance of a broadband (D_2) lamp to infer temperature. Four examples use line-of-sight measurements while the NO-LIF technique (example 3) illustrates the use of fluorescence to infer local laser intensity, and thus extract spatially resolved absorption *T*-measurements.

For the examples of shock-heated CO_2 and the premixed flame independent T information is available to validate the CO_2 absorption thermometry technique. The CO_2 absorption measurements yield values in very good agreement (50–100 K) with the expected result. The predicted T of the detonation experiment is only 100 K above the CO_2 absorption-based temperature that assumes chemical equilibrium. Therefore, we conclude that CO_2 absorption-based determination of gas T has excellent promise for precise gas temperature measurements above 1500 K, including systems with elevated pressure. Three of the examples are at high pressure (premixed flame, pulse detonation engine, and piston engine), and the two engine examples show the utility of this new T diagnostic for time-resolved measurements where p an T vary rapidly in time.

The excellent potential of this temperature diagnostic suggests the value of further research to extend the utility and operating regime of CO_2 UV absorption-based temperature measurement. For the evaluation of detonation temperatures, the absorption cross-sections must be determined up to 4500 K. Measurements for 266 nm are under way and will be reported in a forthcoming publication. Furthermore, the extension of the absorption cross-section database to longer wavelengths (320–400 nm) might provide excellent diagnostics possibilities in long path-length practical combustors.

Acknowledgments

Work at Stanford University was supported by the Air Force Office of Scientific Research, Aerospace Sciences Directorate with Julian Tishkoff as the technical monitor and by the Office of Naval Research with Gabriel Roy as technical monitor. The Division of International Programs at the National Science Foundation supports the Stanford collaboration via a cooperative research grant. The Heidelberg University colleagues (CS & WGB) were sponsored by DFG, DAAD, and BMBF.

References

[1] C. Schulz, J.B. Jeffries, D.F. Davidson, J.D. Koch, J. Wolfrum, R.K. Hanson, *Proc. Combust. Inst.* 29 (2002) 2725–2742.
[2] M. Knapp, A. Luczak, H. Schlüter, V. Beushausen, W. Hentschel, P. Andresen, *Appl. Opt.* 35 (1996) 4009–4017.
[3] W.G. Bessler, M. Hofmann, F. Zimmermann, G. Suck, J. Jakobs, S. Nicklitzsch, T. Lee, J. Wolfrum, C. Schulz, *Proc. Combust. Inst.* 30 (2005), in press.
[4] F. Hildenbrand, C. Schulz, V. Sick, E. Wagner, *Appl. Opt.* 38 (1999) 1452–1458.
[5] W.G. Bessler, C. Schulz, T. Lee, D.I. Shin, M. Hofmann, J.B. Jeffries, J. Wolfrum, R.K. Hanson, *Appl. Phys. B* 75 (2002) 97–102.
[6] F. Hildenbrand, C. Schulz, *Appl. Phys. B* 73 (2001) 165–172.
[7] C. Schulz, J.D. Koch, D.F. Davidson, J.B. Jeffries, R.K. Hanson, *Chem. Phys. Lett.* 355 (2002) 82–88.
[8] W.G. Bessler, C. Schulz, T. Lee, J.B. Jeffries, R.K. Hanson, *Chem. Phys. Lett.* 375 (2003) 344–349.
[9] W.G. Bessler, C. Schulz, T. Lee, J.B. Jeffries, R.K. Hanson, *Appl. Opt.* 42 (2003) 4922–4936.
[10] T.B. Settersten, A. Dreizler, B.D. Patterson, P.E. Schrader, R.L. Farrow, *Appl. Phys. B* 76 (2003) 479–482.
[11] S. Song, R.K. Hanson, C.T. Bowman, D.M. Golden, *Proc. Combust. Inst.* 28 (2000) 2403–2409.
[12] G. Ben-Dor, O. Igra, T. Elperin, *Handbook on Shock Waves.* Academic Press, Boston, 2001.
[13] S.T. Sanders, J.A. Baldwin, T.P. Jenkins, D.S. Baer, R.K. Hanson, *Proc. Combust. Inst.* 28 (2000) 587–594.

[14] S.T. Sanders, D.W. Mattison, J.B. Jeffries, R.K. Hanson, *Shock Waves* 12 (2003) 435–441.
[15] S.T. Sanders, D.W. Mattison, J.B. Jeffries, R.K. Hanson, *Proc. Combust. Inst.* 29 (2002) 2735–2742.
[16] L. Ma, S.T. Sanders, J.B. Jeffries, R.K. Hanson, *Proc. Combust. Inst.* 29 (2002) 161–166.
[17] M.A. Oehlschlaeger, R.K. Hanson, 2003, unpublished data.
[18] D.W. Mattison, M.A. Oehlschlaeger, C.I. Morris, Z.C. Owens, E.A. Barbour, J.B. Jeffries, R.K. Hanson, *Proc. Combust. Inst.* 30 (2005) 2799–2807.
[19] W.G. Bessler, C. Schulz, T. Lee, J.B. Jeffries, R.K. Hanson, *Appl. Opt.* 41 (2002) 3547–3557.
[20] W.G. Bessler, C. Schulz, T. Lee, J.B. Jeffries, R.K. Hanson, *Appl. Opt.* 42 (2003) 2031–2042.
[21] C. Schulz, V. Sick, J. Wolfrum, V. Drewes, M. Zahn, R. Maly, *Proc. Combust. Inst.* 26 (1996) 2597–2604.

Comments

Greg Smallwood, National Research Council Canada, Canada. The fit of the experimental spectra to the theoretical spectra as a function of temperature is best a low wavelengths (<250 nm) but is poor at the longer wavelengths (~300 nm) regardless of the fit temperature. Can you explain this phenomenon? How does this affect the precision of the technique?

Reply. The measurements of the absorption cross section were best for the stronger absorption at shorter wavelength. These measurements were done with a deuterium lamp that also has less intensity at the longer wavelengths. Therefore, the absorption cross section has greater uncertainty for the weaker absorptions at longer wavelength. The potential of the CO_2 absorption technique to determine temperature in high-pressure combustors motivates us to continue our work to improve the accuracy and increase the temperature range of the cross-section measurements. Thus far we have demonstrated the potential of this temperature measurement technique. More work is required to explore the accuracy and precision of this technique.

●

Marcus Aldén, Lund Institute of Technology, Sweden. How would this technique work in a situation with practical fuel that may absorb strongly in the same spectral regions as CO_2?

Reply. For practical fuels, this technique is limited to the post-combustion region where the majority of the fuel has been consumed. Since CO_2 is a major combustion product, in high temperature regions absorption by CO_2 will dominate the absorption by small amounts of unburned fuel. This has been demonstrated in measurements in a Diesel engine that was fueled with commercial Diesel fuel (Ref. [6] in paper). The CO_2 absorption is strongest at high temperature, and thus, the fuel absorption should dominate at low temperature before combustion when the CO_2 concentration is also small. Thus, it is conceivable for the same sensor to monitor fuel in the pre-combustion zone and gas temperature via the CO_2 absorption technique in the post-combustion zone. Work is needed to understand the use of the technique in high-temperature, partially burnt mixtures where the line of sight passes through high temperature CO_2 and significant quantities of unburned fuel.